

Fano resonance and plasmon induced transparency in waveguide-coupled surface plasmon resonance sensors

Shinji Hayashi,^{1,2*} Dmitry V. Nesterenko,¹ and Zouheir Sekkat^{1,3,4}

¹*Optics and Photonics Center, Moroccan Foundation for Science, Innovation and Research (MAScIR), Rabat 10100, Morocco*

²*Department of Electrical and Electronic Engineering, Graduate School of Engineering, Kobe University, Kobe 657-8501, Japan*

³*Department of Chemistry, Faculty of Sciences, University Mohammed V, Rabat 10400, Morocco*

⁴*Department of Applied Physics, Graduate School of Engineering, Osaka University, Suita 585-0871, Japan*
Email: s.hayashi@dragon.kobe-u.ac.jp

A planar multilayer structure that allows coupling between surface plasmon polaritons and waveguide modes is proposed. Calculated reflectivity curves exhibit sharp resonances due to the Fano resonance and plasmon induced transparency arising from the coupling. Electric field profiles obtained at the resonances demonstrate the hybrid nature of the modes excited. When the Fano resonance is used for sensing, the sensitivity with intensity modulation is enhanced by two orders of magnitude relative to that of conventional surface plasmon resonance sensors.

For more than three decades optical sensors based on surface plasmon resonances (SPR) at metallic surfaces have been investigated extensively and SPR sensors have become a central tool for characterizing and quantifying biomolecular interactions.¹⁻⁴⁾ In conventional SPR sensors, it is common to use a Au single layer. However, sensitivity and resolution of the sensors are limited by a broad SPR brought by the Au layer. Various sensor structures have been proposed so far to introduce sharper resonances in the SPR sensor and improve the performance.²⁻⁴⁾ SPR sensors based on the excitation of long-range surface plasmon polaritons (SPP) have been studied extensively by Dostakek et al.⁵⁾ For waveguide (WG)-coupled SPR sensors, in which planar waveguides (PWGs) are integrated in the SPR sensors, sharp resonances have been demonstrated for both the p- and s-polarized incident light originating from the excitation of PWG modes.^{2,3,6)} Recently, Lee et al.⁷⁾ reported on the resolution enhancement in SPR sensors based on metal-insulator-metal multilayer structures.

In recent years, coupling between two electromagnetic modes supported by nanostructures has attracted much interest and has been the subject of intensive theoretical and experimental studies.^{8,9)} It is widely accepted that coupling between a narrow and a broad resonance leads to so-called Fano resonance, characterized by an asymmetric line shape. When the two modes have an identical resonance frequency, coupling results in so-called electromagnetically

induced transparency (EIT), characterized by a sharp transmission band in the middle of a broad absorption band. Although the Fano resonance and EIT have initially been observed in quantum mechanical systems,⁸⁾ they are now known as universal phenomena in various physical systems. EIT-like phenomena realized by plasmonic structures are often called plasmon induced transparency (PIT).^{10,11)} It is also known that the physical nature of the phenomena can be well explained by a classical model of coupled harmonic oscillators.^{9,12,13)} Since the Fano resonance and EIT provides sharp resonances, they may find potential applications in various sensing problems. However, the application of these types of resonance to sensors has not yet been fully explored.

A metal-dielectric interface supports a SPP mode, leading to a broad resonance, and a dielectric PWG structure supports PWG modes, leading to sharp resonances. If these two different types of modes could be successfully coupled, very sharp Fano- and EIT-type resonances are expected to appear. Although WG-coupled SPR sensor structures have already been reported,^{2,3,6)} coupling between the SPP and PWG modes has not been achieved. In the WG-coupled SPR sensor structures reported so far, a dielectric WG layer is placed directly onto the surface of metallic layer. In such a structure, there is no coincidence between the effective indexes of the SPP mode and PWG modes.¹⁾ Consequently, mode coupling is impossible.

In this Letter, we propose a planar structure of WG-coupled SPR sensor that allows the coupling between SPP and PWG modes. Results of numerical calculations clearly demonstrate sharp Fano-type resonance and PIT. A rough estimate indicates that when the light intensity is monitored around the Fano-type resonance, the sensing sensitivity can be enhanced by two orders of magnitude relative to that of conventional SPR.

The structure used for the present simulations is schematically shown in Fig. 1. This is a Kretschmann configuration consisting of a prism, metal layer, first, second and third dielectric layers. When there is only one semi-infinite dielectric layer adjacent to the metal layer, the structure can support SPP modes propagating along the metal-dielectric interface and provides a conventional SPR sensor. On the other hand, when the second dielectric layer (dielectric 2) is surrounded by semi-infinite dielectrics (dielectrics 1 and 3) and the refractive index of dielectric 2 is chosen to be larger than those of dielectrics 1 and 3, the dielectric 2 can support PWG modes. The structure shown in Fig. 1 makes it possible to couple SPP modes with PWG modes when the thickness of dielectric 1 (coupling layer) is chosen appropriately. As in a conventional SPR sensor, the structure can be used as a sensor when light is incident into the prism and the intensity of the reflected light is monitored.

In numerical calculations, we assumed a structure consisting of a prism made of SF10, Au film, Cytop fluopolymer layer as the dielectric 1, high-index ZnS-SiO₂ layer as dielectric 2 and water as dielectric 3. *p*-polarized light with a wavelength of 632.8 nm was assumed to

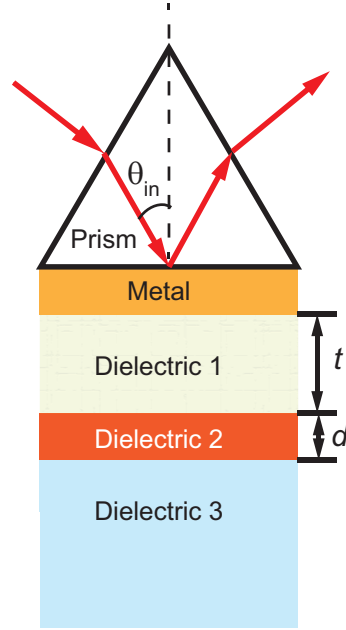


Fig. 1. Structure assumed for simulations.

be incident onto the prism and the reflectivity was calculated as a function of the angle of incidence θ_{in} using a 2×2 transfer matrix method. Values of the refractive indexes used are $n_p = 1.723$ for SF10 prism, $n_{Au} = 0.2184 + i3.5113$ for Au film, $n_{Cy} = 1.340$ for Cytop layer, $n_{WG} = 2.198$ for ZnS-SiO₂ WG and $n_W = 1.332$ for water. The value for the Cytop layer was taken from Ref. 5 and other values were taken from Ref. 7. The thickness of the Au film was fixed at 50 nm, while the thickness of the coupling layer t and that of WG d were taken as free parameters. In the assumed structure, the water acts as a host medium for sensing and the change in the reflectivity curve caused by the change in the refractive index of the medium provides the output of the sensor.

Before proceeding to results of reflectivity calculations we examine the condition for coupling between the SPP and PWG modes. We consider here separately a SPP mode propagating along a semi-infinite Au-Cytop interface and the lowest order transverse magnetic (TM₀) PWG mode supported by a WG surrounded by semi-infinite Cytop and water. In Fig. 2, effective refractive indexes of the SPP and TM₀ PWG modes are plotted as a function of d . A standard equation of the propagation constant of SPP¹⁾ together with the above values of the refractive indexes yields 1.4516 for the effective refractive index of the SPP mode. To obtain the propagation constant of the PWG mode, we used a method based on power dissipation spectra of an oscillating dipole moment placed very close to the WG previously used for multilayer structures.¹⁴⁾ The propagation constant was determined from the position of a peak appearing in the power dissipation spectrum and converted into the effective refractive index. The right ordinate of Fig. 2 indicates the angle of incidence inside the SF10 prism

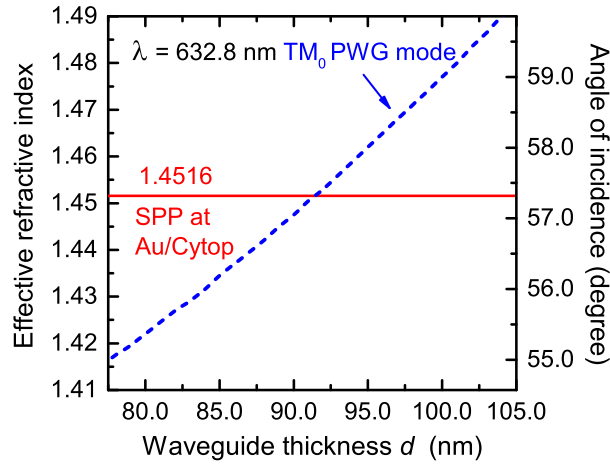


Fig. 2. Effective refractive indexes of SPP and PWG modes.

at which the incident light of 632.8 nm can excite a mode having a corresponding effective refractive index of the left ordinate. We see that the effective refractive index of TM_0 PWG mode increases with increasing d and coincides with that of SPP around $d = 92$ nm. When a WG with this thickness is placed close to the Au surface, coupling between SPP and PWG modes is expected to take place, provided that the effective refractive indexes of the modes remain almost the same when the two structures are brought in close proximity.

Figure 3(a) shows an attenuated-total-reflection (ATR) curve calculated as a function of θ_{in} for a simple Kretschmann configuration consisting of a prism, Au film and Cytop. We see an ATR dip corresponding to the excitation of the SPP mode at the Au-Cytop interface. Figures 3(b), 3(c) and 3(d) present reflectivity curves for the presently proposed structure with $d = 85$, 92 and 100 nm, respectively. To obtain the curves the thickness of the coupling layer was fixed at $t = 700$ nm. For $d = 85$ (Fig. 3(b)) and 100 nm (Fig. 3(d)), we see sharp asymmetric resonances appearing at the low- and high-angle side of the SPP ATR dip. The asymmetric line shape of the resonances is typical of the Fano resonance. The resonance angles coincide well with those of the TM_0 PWG modes for $d = 85$ and 100 nm found in Fig. 2. We can attribute the resonances to the Fano resonance brought by the coupling between the SPP and TM_0 PWG modes. For $d = 92$ nm, the TM_0 PWG mode is tuned to the SPP mode as suggested by Fig. 2 and a sharp peak appears at the middle of the SPP dip (Fig. 3(c)). When Fig. 3(c) is turned upside-down, we get a line shape typical of PIT, i.e., a sharp transmission line inside a broad absorption band. In general, at a SPP ATR dip the energy of incident light is transferred to a SPP and the energy of the SPP is successively dissipated inside a metal. This means that the energy is absorbed by the metal. The appearance of a sharp reflection peak in the SPP ATR dip in Fig. 3 (c) thus implies an appearance of a sharp line of absorption suppression in a broad absorption band, which is the characteristic feature of PIT. Since the

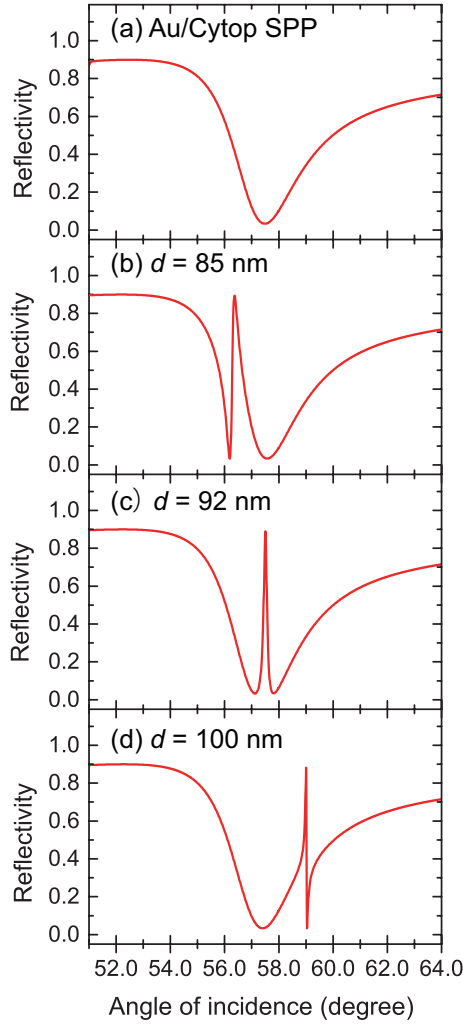


Fig. 3. (a) Reflection dip corresponding to SPP excitation at a Au-Cytop interface. Sharp resonances arising from the coupling between SPP and PWG modes for $t = 700$ nm and $d = 85$ nm (b), 92 nm (c) and 100 nm (d), respectively.

ATR process takes place under the condition of total reflection, there is no transmission of light. However, the line shape seen in Fig. 3(c) can be regarded as the manifestation of PIT caused by the absorption suppression.

Although not shown here, results of our calculations performed with a small imaginary part (1.0×10^{-5}) added to the WG refractive index show that the sharp resonances seen in Figs. 3(b), 3(c) and 3(d) emerge when t becomes smaller than ~ 1000 nm and their amplitudes grow as t decreases. For t smaller than 500 nm, the resonances become broader resulting in two reflection dips which are separated more and more as t decreases. These behaviors of the resonances agree fairly well with general behaviors of coupled oscillators resulting from an increase in the coupling strength.^{12,13} In the present structure, the thickness of the coupling layer determines the strength of coupling between the SPP and PWG modes.

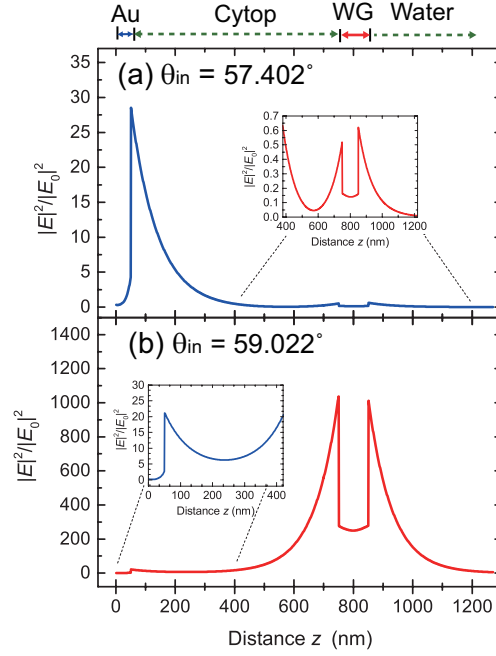


Fig. 4. Electric field profiles (field enhancement factors) for the structure with $d=100$ nm and $t=700$ nm obtained for angles of incidence of 57.402° (a) and of 59.022° (b).

In order to clarify further the origin of the sharp resonances we calculated electric field profiles inside the structure. In Figs. 4(a) and 4(b), results obtained for $d=100$ nm and $t=700$ nm are presented. In the figures, the electric field enhancement factor, which is defined as the ratio of the square of the electric field amplitude to that of the incident light, is plotted as a function of the distance z . The bottom of the prism is taken at $z=0$ nm and we have a Au layer for $0 < z < 50$ nm, coupling layer (Cytop) for $50 < z < 750$ nm, WG for $750 < z < 850$ nm and water for $z > 850$ nm. Figure 4(a) was obtained with $\theta_{in}=57.402^\circ$, which corresponds to the minimum of the SPP reflection dip in Fig. 3(d), while Fig. 4(b) was obtained with $\theta_{in}=59.022^\circ$, which corresponds to the middle of the Fano-type resonance in Fig. 3(d). The inset of Fig. 4(a) represents the region of the WG in an expanded ordinate scale, while that of Fig. 4(b) represents the region close to the Au-Cytop interface. In Fig. 4(a) we see that the strong electric field is generated at the Au-Cytop interface and decays exponentially away from the interface clearly indicating the excitation of the SPP mode. It is important to notice that the electric field profile typical of the PWG mode is also generated in the WG region, although the enhancement factor is smaller than 0.7. In contrast, in Fig. 4(b) we see a strong electric field distribution in the WG region and also a distribution of moderately enhanced electric field near the Au-Cytop interface. It should be noted that the field enhancement factor at the WG-water interfaces is as high as ~ 1000 . The results presented in Figs. 4(a) and 4(b) clearly demonstrate the excitation of hybrid modes of SPP and PWG modes resulting from the coupling.

Figure 4(a) suggests that the decay length of the SPP mode at the Au-Cytop interface is about 150 nm. The interaction of SPP with the PWG mode is believed to be effective only when the WG is placed at a distance shorter than the decay length. However, the result presented in Fig. 4 (b) demonstrates that the PWG mode is strongly excited even when the WG is located at the distance much larger than the decay length. In the present multilayer structure, coupling between the SPP and PWG modes is thought to be caused by the overlap of the evanescent fields associated with the modes, i.e., near-field coupling. In the past, this type of coupling has been studied both experimentally and theoretically for the coupling between SPP modes. Wang¹⁵⁾ has reported efficient photon transport phenomena mediated by near-field coupling of two SPP modes using a double prism configuration. His results demonstrate that the near-field coupling is effective even for a distance much larger than the decay length. Yoshida et al.¹⁶⁾ demonstrated similar phenomena for Ag-SiO₂ multilayer systems. The present result shown in Fig. 4(b) indicates that the near-field coupling between the SPP and PWG modes is also effective at a large distance.

The enhanced electric field associated with the PWG mode can be applied to enhance spectroscopic signals of molecules adsorbed on the WG surface, such as the fluorescence and Raman scattering signals. Furthermore, in exactly the same manner as the conventional SPR sensor, the present structure can be used as a sensor, where the water is used as a sensing medium. In bulk sensing, changes in the refractive index of the whole water caused by dissolution of analytes are detected by monitoring the changes in resonance curves. In thin film sensing, on the other hand, changes in the refractive index and/or thickness of thin films or molecular layers deposited on to the WG surface are detected.

We consider here the bulk sensing and examine the change in the resonance curve caused by the change in the refractive index of water. We chose the structure with $d = 100$ nm and $t = 700$ nm and increase the refractive index of water by an amount of 2.0×10^{-4} . Figure 5 shows the change in the reflectivity curve in an expanded scale for the TM₀ Fano-type resonance. The solid line represents the reflectivity curve before increasing the refractive index of water, which is the same as that presented in Fig. 3(d). As represented by the broken line, the reflectivity curve shifts to higher angles when the refractive index is increased. According to previous papers on the performance of SPR sensors,^{4,17)} the sensitivity with intensity modulation can be estimated by $S_i = \Delta R / \Delta n$, where ΔR is a change in the reflectivity at a fixed angle of incidence caused by a change in the refractive index Δn . For the TM₀ Fano-type resonance shown in Fig. 5, the difference of the two curves ΔR takes a maximum value of 0.3 and leads to $S_i = 1.5 \times 10^3$ RIU⁻¹. Corresponding sensitivities reported for conventional SPR sensors are in the range of a few tens of RIU⁻¹.^{4,17)} The sensitivity with intensity modulation is thus enhanced by two orders of magnitude when the steep part of the Fano-type resonance is used. The present structure is not optimized for sensing, but suggests a huge enhancement

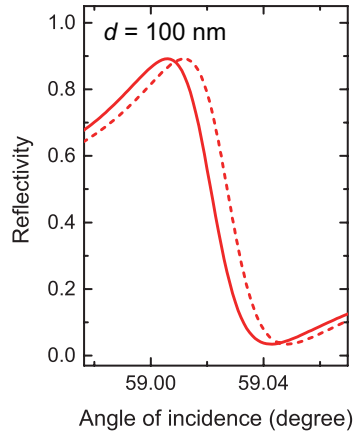


Fig. 5. Shift of the Fano-type resonance for the structure with $d=100$ nm and $t=700$ nm caused by an increase of the refractive index of water $\Delta n = 2.0 \times 10^{-4}$.

in the sensitivity achieved by the Fano-type resonance. The optimization of the structure and a systematic estimation of sensitivity and resolution is now under way in our group and the results will be published elsewhere.

In summary, a planar multilayer structure that allows coupling between SPP and PWG modes is proposed. Results of reflectivity calculations demonstrate clearly sharp Fano-type resonance and PIT appearing in the region of the reflectivity dip of SPP excitation. The calculated electric field profiles demonstrate the hybrid nature of the electromagnetic modes excited in the present structure. A rough estimate of sensing sensitivity with intensity modulation indicates that the Fano-type resonance leads to a sensitivity enhancement by two orders of magnitude relative to that of conventional SPR. In practical applications, the presently proposed structure can be constructed by a variety of dielectrics and sharp resonances can be obtained when the refractive indexes and the thicknesses of the dielectrics are properly chosen. Simulations with a variety of dielectrics and experimental observation of the sharp resonances are currently under way in our laboratory and the results will be published elsewhere. At the Fano resonance and PIT, the present structure induces very high electric field enhancements at the WG-water interface. This implies that the structure can also be applied to enhance Raman scattering and fluorescence of molecules placed very close to the WG-water interface.

Acknowledgements This work was partially supported by JSPS KAKENHI Grant Number 23310064 and Osaka University International Joint Research Promotion Program.

References

- 1) H. Raether, *Surface plasmons on smooth and rough surfaces and on gratings*, Springer tracts in modern physics, **111** (Springer-Verlag, 1988).
- 2) W. Knoll, *Annu. Rev. Phys. Chem.* **49**, 569 (1998).
- 3) J. Homola, *Chem. Rev.* **108**, 462 (2008).
- 4) J. Homola, S. S. Yee, and G. Gauglitz, *Sensors and Actuators B* **54**, 3 (1999).
- 5) J. Dostalek, A. Kasry, and W. Knoll, *Plasmonics* **2**, 97 (2007).
- 6) Z. Salamon, H. A. Macleod, and G. Tollin, *Biophys. J.* **73**, 2791 (1997).
- 7) K-S. Lee, J. M. Son, D-Y. Jeong, T. S. Lee, and W. M. Kim, *Sensors* **10**, 11390 (2010).
- 8) B. Luk'yanchuk, N. I. Zheludev, S. A. Maier, N. J. Halas, P. Nordlander, H. Giessen, and C. T. Chong, *Nature Mater.* **9**, 707 (2010).
- 9) A. E. Miroshnichenko, S. Flach, and Y. S. Kivshar, *Rev. Mod. Phys.* **82**, 2257 (2010).
- 10) S. Zhang, D. A. Genov, Y. Wang, M. Liu and X. Zhang, *Phys. Rev. Lett.* **101**, 047401 (2008).
- 11) J. Zhang, W. Bai, L. Cai, Y. Xu, G. Song, and Q. Gan, *Appl. Phys. Lett.* **99**, 181120 (2011).
- 12) G. L. Garrido Alzar, M. A. G. Martinez, and Nussenzveig, P., *Am. J. Phys.* **70**, 37 (2002).
- 13) Y. S. Joe, A. M. Satanin, and C. S. Kim, *Phys. Scr.* **74**, 259 (2004).
- 14) S. Hayashi, A. Maekawa, S. C. Kim, and M. Fujii, *Phys. Rev. B* **82**, 035441 (2010).
- 15) Y. Wang, *Appl. Phys. Lett.* **82**, 4385 (2003).
- 16) M. Yoshida, S. Tomita, H. Yanagi, and S. Hayashi, *Phys. Rev. B* **82**, 045410 (2010).
- 17) D. V. Nesterenko and Z. Sekkat, *Plasmonics* **8**, 1585 (2013).